



Cationic iridium complexes of the Xantphos ligand. Flexible coordination modes and the isolation of the hydride insertion product with an alkene

Ashley J. Pontiggia, Adrian B. Chaplin, Andrew S. Weller*

Department of Chemistry, Inorganic Chemistry Laboratory, University of Oxford, Oxford, OX1 3QR, UK

ARTICLE INFO

Article history:

Received 14 January 2011

Received in revised form

28 January 2011

Accepted 28 January 2011

Keywords:

Iridium

Phosphine

Pincer

X-ray

Hydride

Xantphos

ABSTRACT

Reaction of the Ir(I)–Xantphos complex $[\text{Ir}(\kappa^2\text{-Xantphos})(\text{COD})][\text{BAr}^{\text{F}}_4]$ (Xantphos = 4,5-bis(diphenylphosphino)-9,9-dimethylxanthene, $\text{Ar}^{\text{F}} = \text{C}_6\text{H}_3(\text{CF}_3)_2$) with H_2 in acetone or $\text{CH}_2\text{Cl}_2/\text{MeCN}$ affords the Ir(III)–hydrido complexes $[\text{Ir}(\kappa^3\text{-Xantphos})(\text{H})_2(\text{L})][\text{BAr}^{\text{F}}_4]$, L = acetone or MeCN, whereas in non-coordinating CH_2Cl_2 solvent dimeric $[\text{Ir}(\kappa^3\text{-Xantphos})(\text{H})(\mu\text{-H})_2][\text{BAr}^{\text{F}}_4]_2$ is formed. A common intermediate in these reactions that invokes a $(\sigma, \eta^2\text{-C}_8\text{H}_{13})$ ligand is reported. Addition of excess tert-butylethene (tbe) to $[\text{Ir}(\kappa^3\text{-Xantphos})(\text{H})_2(\text{MeCN})][\text{BAr}^{\text{F}}_4]$ results in insertion of a hydride into the alkene to form $[\text{Ir}(\kappa^3\text{-Xantphos})(\text{MeCN})(\text{CH}_2\text{CH}_2\text{C}(\text{CH}_3)_3)(\text{H})][\text{BAr}^{\text{F}}_4]$, an Ir(III) alkyl–hydrido–Xantphos complex. This reaction is reversible, and heating (80 °C) results in the reformation of $[\text{Ir}(\kappa^3\text{-Xantphos})(\text{H})_2(\text{MeCN})][\text{BAr}^{\text{F}}_4]$ and tbe. These complexes have been characterised by NMR spectroscopy, ESI-MS and single-crystal X-ray diffraction. They show variable coordination modes of the Xantphos ligand: *cis*- $\kappa^2\text{-P,P}$, *fac*- $\kappa^3\text{-P,O,P}$ and *mer*- $\kappa^3\text{-P,O,P}$ with the later coordination mode like that found in related PNP–pincer complexes.

© 2011 Elsevier B.V. All rights reserved.

1. Introduction

Transition-metal complexes involving tridentate “pincer” ligands, especially with the later transition metals, are an important class of materials as they mediate many interesting, and contemporary, transformations such as the activation of E–H bonds [1–4]. Within the complexes of group 9 metals, those with formally neutral PNP-type ligands (Chart 1) are distinct from (formally anionic) PCP-type ligands as they often result in an overall positive charge on the metal centre. In this regard they are similar to POP-type ligands such as DPEphos and Xantphos that have found application in a number of catalytic processes, especially carbonylation reactions such as hydroformylation [5–7]. Xantphos (Chart 1) is a particularly interesting comparison, as it is relatively rigid and thus might be expected to coordinate in a manner similar to PNP–ligands [8,9]. However well-characterised P,O,P- κ^3 -coordination modes of Xantphos are, surprisingly, rare, there being only a handful of fully characterised examples [8–12]. The P,P- κ^2 -coordination mode (*i.e.* with the O–donor atom not bound) is far more common. We have recently reported upon this unusual κ^3 coordination mode using Rh-based systems, *e.g.* A [13], and were interested in extending this to iridium to afford complexes that are directly analogues to Ir–PNP systems that have found much recent

application in C–H activation chemistry [14–18]. We report here a preliminary study into their synthesis and reactivity.

2. Results and discussion

Complex **1** $[\text{Ir}(\kappa^2\text{-Xantphos})(\text{COD})][\text{BAr}^{\text{F}}_4]$ (COD = 1,5-cyclooctadiene, $\text{Ar}^{\text{F}} = \text{C}_6\text{H}_3(\text{CF}_3)_2$) that is the precursor to the studies reported here is readily synthesised by addition of Xantphos to $[\text{Ir}(\text{COD})\text{Cl}]_2$ in CH_2Cl_2 solvent in the presence of the halide abstracting agent $\text{Na}[\text{BAr}^{\text{F}}_4]$ Scheme 1. X-ray quality crystals of dark orange **1** allowed for the solid-state structure to be determined, as shown in Fig. 1. This demonstrates a pseudo-square planar environment around the Ir(I) centre with *cis* phosphines and an oxygen atom that is not coordinated with the metal ($\text{Ir1}\cdots\text{O1}$, 2.544(2) Å). Although the coordination environment is distorted somewhat from being ideal square planar, with the Ir–P distances differing by 0.1 Å and the COD ligand twisted [planes defined by P1–Ir1–P2 and the Ir1–centroid(C1,C2)–centroid(C5,C6) 21.99(3)°] the cation approximates to C_s symmetry in the solid-state. Other *cis*- κ^2 -Xantphos complexes have been structurally characterised [10,19–22]. In contrast to the solid-state structure, in solution the ^1H NMR spectrum of **1** shows equivalent methyl protons (δ 1.75, 6H) at room temperature and a single alkene COD environment (δ 3.85, 4H), *i.e.* apparent C_{2v} symmetry. The ^{31}P $\{^1\text{H}\}$ spectrum shows a singlet at δ 14.26 demonstrating equivalent phosphine environments. These data are consistent with rapid inversion of the

* Corresponding author.

E-mail address: andrew.weller@chem.ox.ac.uk (A.S. Weller).

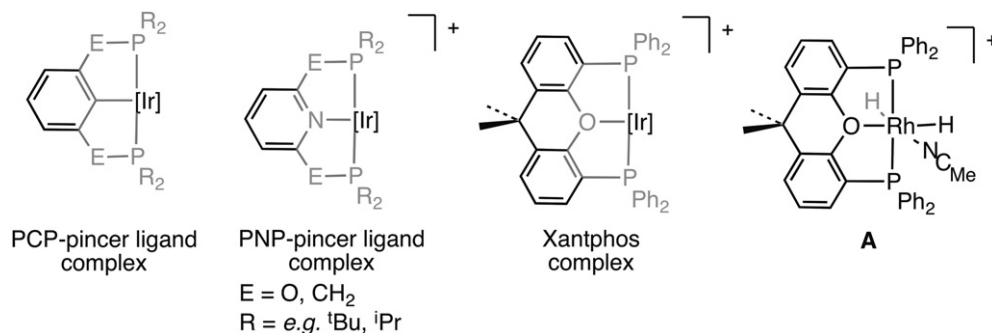


Chart 1.

Xantphos ligand on the NMR timescale in solution, possibility via a κ^3 -intermediate [12]. Similar NMR data are observed for the analogous Rh–norbornadiene complex [13].

Addition of hydrogen (~4 atm) to **1** in *d*₆-acetone solution resulted in a colour change from orange to colourless, and ultimately (24 h) affords the dihydride complex [Ir(κ^3 -Xantphos)(H)₂(acetone)][BARF₄], **3**, and the hydrogenation of COD to cyclooctane (COA). Initially formed, however, is an intermediate, spectroscopically characterised *in situ* as the mono-hydrido complex [Ir(κ^3 -Xantphos)(H)(σ , η^2 -C₈H₁₃)][BARF₄] **2** (Scheme 2). The ¹H NMR spectrum of the reaction mixture after 10 min shows this intermediate to be the dominant species in solution. Two alkene peaks at δ 4.94 and 4.24 that integrate each to 1H relative to [BARF₄] and a doublet of doublets at δ -7.28 (dd, 1H) that shows *cis* couplings to the phosphines ($J(\text{PH}) = 17.9, 27.5$ Hz) are observed. This hydride signal collapses into a singlet on decoupling ³¹P. Two Xantphos methyl environments are observed (δ 1.99, 1.41). The alkene peaks correlate with each other (COSY) and also to signals at 84.4 and 76.3 in the ¹³C {¹H} NMR spectrum (HSQC) which lie in the region associated with bound alkene ligands. A relatively high frequency signal in the ¹H NMR spectrum (δ 3.58) does not couple with the alkene peaks (COSY) and shows a strong correlation to a carbon signal at 16.1. This carbon signal is also the lowest frequency one in the ¹³{¹H} NMR spectrum and shows no correlation to other protons, suggesting an Ir–CHR₂ group. The ³¹P {¹H} spectrum shows a pair of AB-roofed doublets (δ 7.4, 3.2) with a magnitude of coupling constant that demonstrates *trans*-orientated phosphines ($J(\text{PP}) = 288$ Hz). ESI-MS (ElectroSpray Ionisation-Mass Spectrometry) demonstrates the dominant parent ion at $m/z = 881.267$ ([IrC₄₇H₄₆P₂O₁]⁺ calc. 881.265) that fits the suggested formulation. These data are fully consistent with partial hydrogenation of COD to form a (σ , η^2 -C₈H₁₃) ligand. These data also argue against alternative formulations as an allyl [23–25] or vinyl [17] ligands. The formation of a σ , η^2 -C₈H₁₃ ligand from insertion of a hydride into a coordinated COD ligand has been reported previously [26,27].

Over a period of 24 h compound **2** smoothly converts to a new compound, characterised as [Ir(κ^3 -Xantphos)(H)₂(acetone)][BARF₄], **3**. The ³¹P {¹H} spectrum of **3** shows a single environment at δ 32.26 as a singlet, while two hydride environments are observed in the ¹H NMR spectrum at δ -26.01 and -26.90, both of which are

doublets of triplets, collapsing to doublets on decoupling ³¹P. The coupling constants show *cis* ¹H–³¹P coupling ($J(\text{PH}) = 13.8$ and 14.0 Hz respectively), with no *trans* coupling observed. Inequivalent Xantphos methyl protons (δ 1.99 and 1.77) and free C₈H₁₆ (δ 1.52) were also observed. There is no indication of any COD alkene or allyl signals in the range δ 3–5. These data point towards a structure for **3** as shown in Scheme 2. We assign the remaining coordination site to be occupied by a molecule of solvent (acetone). Similar structures have been reported for Rh [13] and Ru [8] Xantphos complexes while the close chemical shift of the hydrides points to a similar *trans* donor atom (*i.e.* O) for each. Strong peaks observed by ESI-MS at $m/z = 831.208$ ([IrC₄₂H₄₀O₂P₂]⁺ calc. 831.213) and 773.168 ([M]⁺ – acetone, calc. 773.171) support this formulation. We were unable to isolate crystalline samples of either **2** or **3** and thus neither a solid-state structural determination nor micro-analytical data were obtained. Nevertheless spectroscopic and ESI-MS data are unequivocal for their determination.

Repeating the hydrogenation in very weakly-coordinating solvent CD₂Cl₂ with an added 2 eq of MeCN (per **1**) led to the formation of a new colourless complex [Ir(κ^3 -Xantphos)(H)₂(MeCN)][BARF₄] **4** after 24 h, which was characterised by NMR spectroscopy, ESI-MS, and a single-crystal X-ray diffraction experiment (Scheme 3). The NMR data of **4** are very similar to those

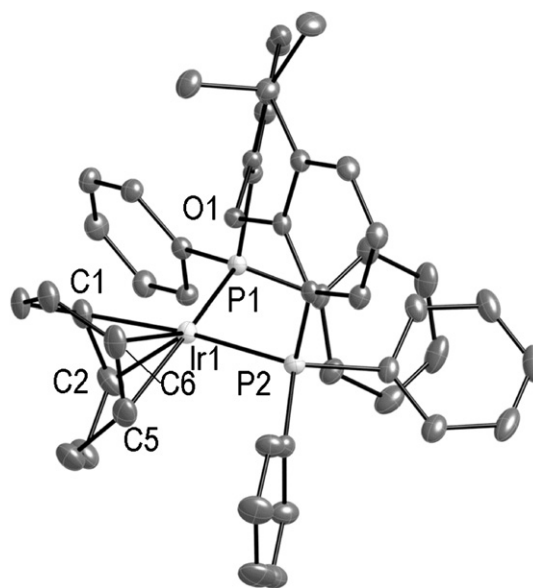
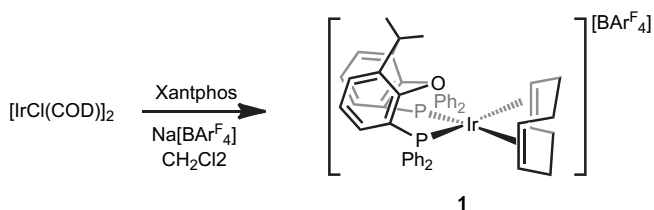
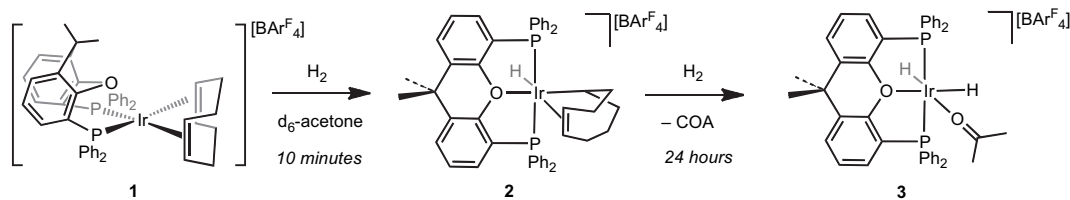


Fig. 1. The molecular crystal structure of the cationic portion of **1**, only the major disordered component of the COD ligand shown. Hydrogen atoms and anion are omitted for clarity. Thermal ellipsoids are shown at the 30% probability level. Selected bond distances (Å): Ir1–P1, 2.3258(8); Ir1–P2, 2.4209(9); Ir1–C1, 2.161(4); Ir–C2, 2.161(4); Ir1–C5, 2.300(4); Ir1–C6, 2.208(4); Ir⋯O1, 2.544(2). Selected angle (°): P1–Ir1–P2, 101.22(3).



Scheme 1.



Scheme 2.

of **3**. The ^1H NMR spectrum of isolated material demonstrates two hydride environments at $\delta -18.55$ and -26.79 both of which are doublets of triplets, $J(\text{PH}) = 12.8, 15.4$ Hz respectively, and show a mutual $^1\text{H}-^1\text{H}$ coupling of $J(\text{HH}) = 7.4$ Hz. Although similar to **3**, the larger chemical shift dispersion for the hydrides in **4** reflects different *trans* ligands (O and N) and we assign the signal at $\delta -18.55$ to the hydride *trans* to the acetonitrile ligand [28]. In the alkyl region of the spectrum peaks for coordinated acetonitrile ($\delta 1.90$) and inequivalent Xantphos methyl protons ($\delta 1.50$ and 1.18) are observed. The $^{31}\text{P}\{^1\text{H}\}$ NMR spectrum shows a single environment at $\delta 27.97$. ESI-MS shows a peak at $m/z = 814.196$ ($[\text{C}_{41}\text{H}_{37}\text{P}_2\text{NOIr}]^+$ calc. 814.198). These data are consistent with the formation of an acetonitrile analogue of the Xantphos acetone adduct **4** in which the Xantphos ligand is *trans* spanning and the acetonitrile ligand is bound *trans* to a hydride. The solid-state structure of **4** is shown in Fig. 2 and confirms the coordination geometry as determined by NMR spectroscopy. In particular it demonstrates a P–Ir–P bond angle of $164.10(4)^\circ$, and a MeCN ligand *trans* to a hydride. As seen for the formation of **3**, the intermediate **2** was observed during the initial stages of the reaction. Addition of acetone (ca. 2 eq) to a CD_2Cl_2 solution of **4** resulted in a mixture of **3** and **4** in a 1:5 ratio respectively. This demonstrates exchange of the bound MeCN ligand, which at the 18-electron Ir(III) centre must be *via* a dissociative process. Complexes **3** and **4** are directly analogous to PNP-type pincer complexes [14–16,18], such as $[\text{Ir}(\text{PNP})(\text{H})_2(\text{NCMe})][\text{BF}_4]$ [17] (PNP = [2,6-bis-(di-tert-butylphosphinomethyl)pyridine]).

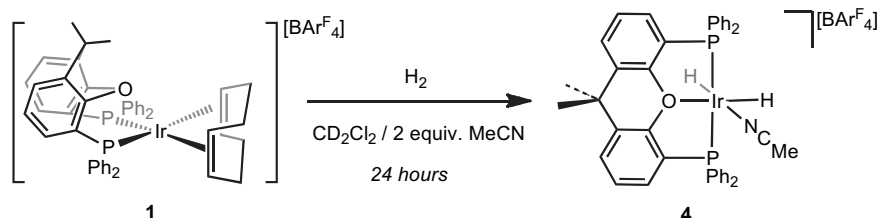
In contrast to the hydrogenation of **1** in acetone or $\text{CH}_2\text{Cl}_2/\text{MeCN}$ solvents, both of which are relatively coordinating and reveal final products that have coordinated solvent, hydrogenation in CD_2Cl_2 forms a bi-metallic complex with no coordinated solvent: $[\text{Ir}(\kappa^3\text{-Xantphos})(\text{H})(\mu\text{-H})_2][\text{BARF}_4]_2$, **5** (Scheme 4), as characterised by NMR spectroscopy, X-ray crystallography and ESI-MS. Complex **2** was once again observed as an intermediate, which changed smoothly to **5** over 24 h. The ^1H NMR spectrum of **5** showed two sets of Xantphos methyl protons at $\delta 2.16$ and 2.14 . Complex second-order multiplets observed at $\delta -6.68$ and -22.81 , both integrating as 2H, are assigned to the hydrides. The former resonance is characteristic in both chemical shift and coupling constants for hydride ligands that bridge two metal centres, while the latter is characteristic for terminal hydrides. Line-shape analysis of these hydride resonances in an AA'BB'XX'X''X''' system gave a satisfactory, if not perfect fit, and reveals a coupling constant between the bridging hydride ($\delta -6.68$) and the phosphine of ~ 64 Hz suggesting a *trans* orientation, while the other

couplings, especially those to the hydride signal at $\delta -22.81$, are much smaller (<20 Hz) indicative of *cis*-coupling. In the $^1\text{H}\{^{31}\text{P}\}$ spectrum these hydride multiplicities reduce to two simple triplets with $J(\text{HH}) = 3.4$ Hz. The $^{13}\text{C}\{^1\text{H}\}$ NMR spectrum shows a single environment for $\text{C}(\text{CH}_3)_2$ while two environments for $\text{C}(\text{CH}_3)$ are observed. The $^{31}\text{P}\{^1\text{H}\}$ NMR spectrum shows a single environment at $\delta 22.90$. These data suggest a ratio of Xantphos ligand to hydrides of 1:2, and a rather symmetric structure. The dimeric formulation of **5** was revealed by ESI-MS which showed $m/z = 773.180$ ($[\text{C}_{78}\text{H}_{68}\text{P}_4\text{O}_2\text{Ir}_2]^{2+}$ calc. 773.171) consistent with a dimer with a +2 charge, that is to say an increase between each isotopomer of $m/z = 0.5$ and an overall isotope pattern that clearly indicated a dimeric $\{\text{Ir}_2\}^{2+}$ formulation.

These data point to a formulation for **5** which is a centrosymmetric dimer with bridging hydrides. A crystal structure determination confirmed this to be the case (Fig. 3), showing the Xantphos ligand binding in as κ^3 – with a facial coordination geometry, the oxygen coordinating to the Ir(III) centre (Ir1–O1, 2.220(3) Å). This distance is not appreciably different from that found for the κ^3 – meridional binding mode (e.g. **4** and **6**, vide infra). The hydride ligands were not located in the final difference map, but an apparent vacant site in the coordination sphere *trans* to O1 is the likely location of the terminal hydride, while the bridging hydrides sit *trans* to P1 and P2, consistent with the NMR data. The Ir–Ir distance of 2.6460(4) Å is consistent with a formal twice protonated M=M double bond, or alternatively an 18-electron configuration can be obtained by treating each bridging hydride as a 3-centre 2-electron bond. The bonding in such dimeric species has been discussed previously [29]. Similar structures for Ir_2 dimeric species with bridging hydrides have been reported, which show similar Ir–Ir separations [23,30]. As far as we are aware **5** is the first crystallographically characterised example of a κ^3 -Xantphos ligand with facial coordination geometry. Changes in coordination geometry from κ^3 -fac to κ^3 -mer have previously been observed in related Rh-complexes of DPEphos [31].

The synthesis of **5** on a large scale (>10 mg) proved problematic as hydrogenation in CH_2Cl_2 led to trace impurities that could not be removed by recrystallisation. However, addition of H_2 to **1** in fluorobenzene ($\text{C}_6\text{H}_5\text{F}$) solvent resulted in the clean formation of **5** and allowed its isolation in a yield of 53% as bright orange crystals that precipitated out of solution as analytically pure material.

Addition of MeCN to complex **5** resulted in the quantitative formation of **4** after 2 h. A deep-red intermediate was observed in the early stages of the reaction, but this was short lived and we



Scheme 3.

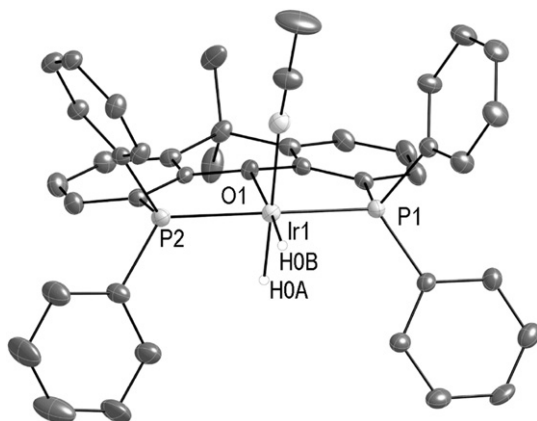


Fig. 2. The molecular crystal structure of the cationic portion of **4**. Hydrogen atoms, apart from the hydrides, and anion are omitted for clarity. Hydride ligands were located in the difference Fourier map. Thermal ellipsoids are shown at the 30% probability level. Selected bond distances (Å): Ir1–P1, 2.2649(11); Ir1–P2, 2.2771(11); Ir–O1, 2.249(3); Ir–N1, 2.105(4). Selected angles (°): P1–Ir1–P2, 164.10(4); O1–Ir1–N1, 95.86(12).

have not been able to definitely characterise it. NMR spectroscopy after 15 min shows a broad environment in the $^{13}\text{P}\{^1\text{H}\}$ NMR spectrum at δ 0.1 ppm, while in the hydride region in the ^1H NMR spectrum a very broad (fwhm \sim 500 Hz) and sharper (fwhm \sim 40 Hz) set of signals are observed at δ –11 and δ –17.1 respectively, of approximate equal intensity. Given the similarity of this data to **5** we tentatively assign this complex as the MeCN adduct of the dimer **5** in which the Xantphos ligand remains *cis* coordinated but the oxygen is no longer bound (Scheme 5).

A well-reported hydrogen acceptor is tert-butylethene (tbe), which has found considerable use in the generation of active, low-coordinate, Ir(I) species from Ir(III)–hydrido complexes [32]. When tbe was added in excess to the dimeric **5** in CD_2Cl_2 solvent no reaction was observed after 4 days, even on mild heating (40 °C). This possibly suggests that the does not break up the dimeric structure, unlike MeCN (*i.e.* **5** to **4**). In contrast, addition of an excess of tbe to the monomeric acetonitrile adduct **4** in CD_2Cl_2 resulted in the formation of a new species, which was the sole-product after 20 h. No intermediates were observed, with **4** cleanly transforming into the new product. In the ^1H NMR spectrum a triplet at δ –18.20 (1H) with a *cis* ^1H – ^{31}P coupling constant of $J(\text{PH}) = 15.2$ Hz, a singlet at δ 0.55 that integrated as 9H is assigned to the ^tBu group and two methyl environments for the Xantphos ligand were observed. Signals assigned to methylene groups at δ 1.93 and 1.02 (2H each) were seen, while no signals characteristic to a coordinated tbe ligand [33,34] or a vinyl ligand (*i.e.* Ir–CH=CHR) [35–38] were observed. The $^{31}\text{P}\{^1\text{H}\}$ NMR spectrum only showed a singlet at δ 21.34, which in combination with the other spectroscopic data, suggests a *trans* conformation of the Xantphos ligand. These data suggest that tbe coordination and hydride insertion have occurred to give an alkyl hydride. ESI-MS showed the dominant parent ion as

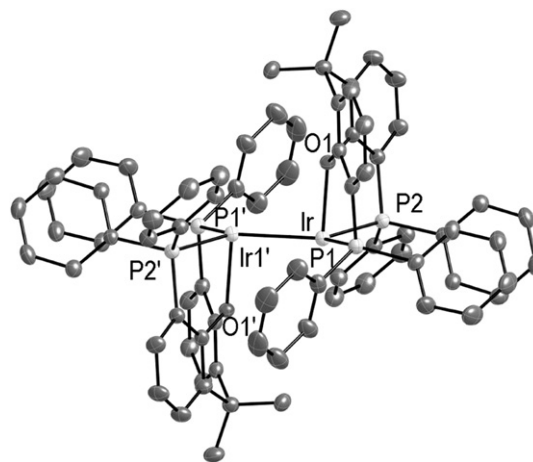
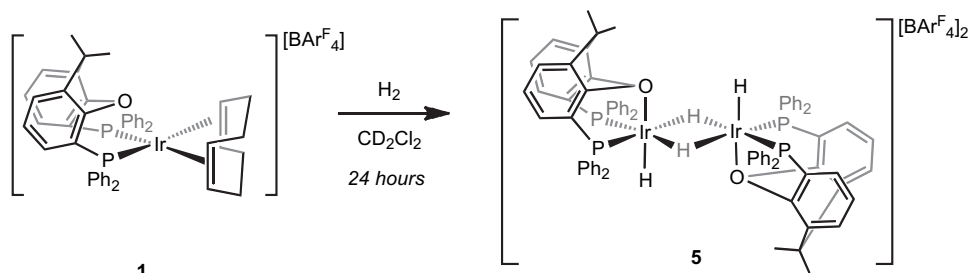


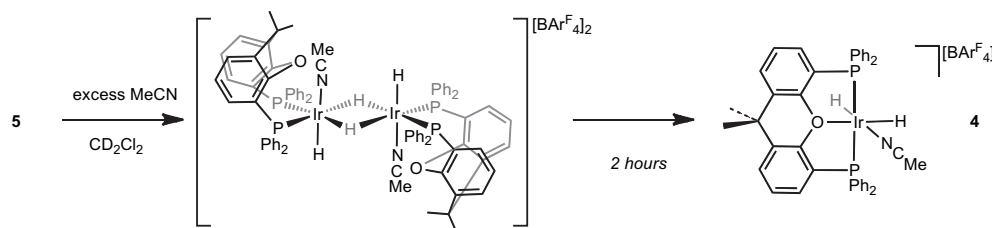
Fig. 3. The molecular crystal structure of the cationic portion of **5**. Hydrogen atoms are omitted for clarity. The hydride atoms were not located in the difference Fourier map. Selected bond distances (Å): Ir1–P1, 2.2827(13); Ir1–P2, 2.2461(14); Ir–O1, 2.220(3); Ir1–Ir', 2.6460(4). Selected Angles (°): P1–Ir1–P2, 105.24(5); O1–Ir1–P1, 82.34(9); O1–Ir1–P2, 82.74(10).

$m/z = 898.291$ ($[\text{IrC}_{47}\text{H}_{49}\text{O}_2\text{P}_2]^+$ calc. 898.29, *i.e.* **4** + tbe), which is consistent with this. A crystal structure confirmed the structure as $[\text{Ir}(\kappa^3\text{-Xantphos})(\text{MeCN})(\text{CH}_2\text{CH}_2\text{C}(\text{CH}_3)_3)(\text{H})][\text{BAR}^{\text{F}}_4]$ **6** (Scheme 6, Fig. 4). Key structural metrics that identify the alkyl hydride are the C1–C2 distances 1.495(8) Å, that identifies it as a C–C single bond rather than a C=C double bond (*c.f.* 1.30(1) Å in *trans*-Ir{(CH=CHC(CH₂CH₂Ph)₂CH₃)(CO)(PPh₃)₂} [37] and 1.299(7) Å in Tp/Rh(CNneo)(CH=CHCMe₃)Cl [38]), and that the Ir1–C1–C2 angle (116.8(4)°) is also much smaller than expected for a vinyl group (\sim 130° [38]). The hydride ligand was located in the final difference map and sits *trans* to the MeCN ligand.

In **6** the tbe ligand has undergone insertion into one of the hydride ligands in **4**, presumably *via* dissociation of the MeCN ligand (as suggested in the reaction with acetone), alkene coordination and hydride migration. The formation of the linear product is consistent with insertion favouring the least sterically crowded complex. Related Iridium(III)–PNP [15,39] and Iridium(III)–PCP[40,41] pincer complexes that are alkyl, aryl or vinyl–hydrido species have been reported previously. A characteristic reactivity profile of these is reductive elimination of alkane, arene or alkene respectively to give Ir(I) species, that themselves can often undergo oxidative addition [14,15,40,41]. On heating **6** in $\text{C}_6\text{H}_5\text{F}$ solvent at 80 °C for 2 h we see no evidence for the formation of a stable Ir(I) species, however under these conditions complex **4** is reformed cleanly alongside 1 eq of tbe (by ^1H NMR spectroscopy). A likely mechanism is reversible dissociation of MeCN and β -elimination from the alkyl group to reform tbe. Given this observation, presumably it is the excess tbe used in the synthesis of **6** from **4** that provides the driving force for its formation.



Scheme 4.



Scheme 5.

3. Conclusions

Cationic κ^3 -pincer-type complexes of Ir(III)-dihydrides have been synthesised from reaction of a precursor Ir(I)-Xantphos complex. These complexes show variable coordination modes of the Xantphos ligand: *cis*- κ^2 -P,P, *fac*- κ^3 -P,O,P and *mer*- κ^3 -P,O,P; with the last coordination mode like that found in PNP-pincer complexes. Related to this analogy, an alkyl-hydrido-Xantphos complex has been isolated from reaction of a dihydride with an alkene (tbe), that is closely related to alkyl-hydrido-PNP species that are precursor complexes for C–H activation process by Ir(I) reactive intermediates. The formation of this complex is reversible, and heating isolated material reforms the dihydride and alkene. The coordination chemistry of Xantphos thus shows very interesting parallels with that of PNP-ligands [8,9], with the added spice of having flexible coordination modes. It will be interesting to see whether these facets can be harnessed in catalytic cycles that are also mediated by PNP-type complexes.

4. Experimental

All manipulations were carried out under an atmosphere of Argon using standard Schlenk and glove-box techniques. Glassware was oven dried at 130 °C overnight and flamed under vacuum prior to use. Unless otherwise stated, all solvent reagents were placed under an Argon atmosphere before use using three freeze–pump–thaw cycles. Dichloromethane, acetonitrile, pentane and hexane were dried using a Grubbs-type solvent purification system (MBraun SPS-800) [42]. Acetone and d_6 -acetone were stirred over 3 Å molecular sieves overnight then distilled under vacuum. CD_2Cl_2 , and C_6H_5F were distilled under vacuum from CaH_2 and stored over 3 Å molecular sieves. The Xantphos ligand was used as purchased from Sigma–Aldrich. $Na[BAr^F_4]$ and $[Ir(cod)Cl]_2$ were prepared according to published literature methods or variations thereof. [43,44] NMR spectra were recorded on Varian 500 MHz, Bruker 500 MHz and Varian 300 MHz spectrometers. Chemical shifts are quoted in ppm and coupling constants in Hz. ESI-MS was carried out on a Bruker MicroTOF instrument interfaced to a glove box [45]. Samples were diluted with the appropriate solvent before being injected via a gas-tight syringe. Microanalyses were performed by Elemental Micro-analysis Ltd.

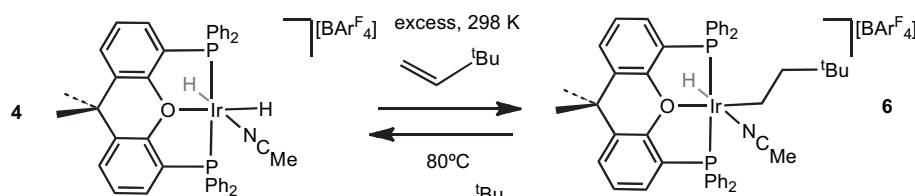
5. Crystallography

Relevant crystallographic data are given in Table 1. Data was acquired on an Enraf Nonius Kappa CCD diffractometer using graphite monochromated Mo $K\alpha$ radiation ($\lambda = 0.71073$ Å) and a low-temperature device (150 K); data was collected using COLLECT, reduction and cell refinement was performed using DENZO/SCALEPACK [46,47]. Structures were solved by direct methods using SIR2004 (1, 4, 6) or by Patterson interpretation using SHELXS-86 (5), and refined full-matrix least squares on F^2 using SHELXL-97 [48,49]. All non-hydrogen atoms were refined anisotropically. Hydride ligands were located in the difference Fourier map for complexes 4 and 6. Problematic solvent disorder in the structure of 5 and 6 was treated using the SQUEEZE algorithm [50]. Further details of disorder modelling are documented in the crystallographic information files under the heading `_refine_s-pecial_details`. Restraints to thermal parameters were applied were necessary in order to maintain sensible values.

5.1. $[Ir(\kappa^2\text{-Xantphos})(COD)][BAr^F_4]$ 1

A solution of Xantphos (169.7 mg, 0.29 mmol) in CH_2Cl_2 (3 mL) was added dropwise to a stirred CH_2Cl_2 (6 mL) suspension of $[Ir(cod)Cl]_2$ (98.5 mg, 0.15 mmol) and $Na[BAr^F_4]$ (260.6 mg, 0.29 mmol). The dark orange solution was then stirred at ambient temperature for a further 2 h. The solution was filtered *via* cannula and the solvent removed *in vacuo* to yield a dark orange solid, which was recrystallised from CH_2Cl_2 /pentane. Yield: 398.1 mg (78.0%). Crystals suitable for X-ray diffraction were obtained by recrystallisation from CH_2Cl_2 /pentane at room temperature.

1H (500 MHz, CD_2Cl_2 , 298 K): δ 7.72 (s, 8H, BAr^F_4), 7.61 (m, 2H, phenyl), 7.56 (s, 4H, BAr^F_4), 7.37 (8H, m, aryl), 7.24 (m, 16H, aryl), 3.85 (s, 4H, cod), 1.75 (s, 6H, CH_3), 1.72 (m, 4H, cod), 1.35 (m, 4H, cod). ^{31}P { 1H } NMR (202 MHz, CD_2Cl_2 , 298 K): δ 14.26 (s). ^{13}C { 1H } (125 MHz, CD_2Cl_2 , 298 K): δ 162.31 (q, $J_{CB} = 49.6$, BAr^F_4), 161.48 (d, $J_{CP} = 4.3$, aryl), 137.72 (d, $J_{CP} = 5.7$, aryl), 135.36 (s, BAr^F_4), 133.79 (s, aryl), 132.57 (d, $J_{CP} = 11.4$, phenyl), 132.04 (dd, $J_{CP} = 43.9$, 2.86, P-C_{phenyl}), 131.16 (s, aryl), 129.42 (d, $J_{CP} = 10.5$, phenyl), 129.41 (qq, $J_{CF} = 32$, 2.8, BAr^F_4), 129.14 (s, aryl), 128.62 (d, $J_{CP} = 5.7$, aryl), 125.25 (q, $J_{CF} = 272.7$, BAr^F_4), 124.37 (d, $J_{PC} = 42.9$, P-C_{aryl}), 124.07 (s, aryl), 118.04 (sept, $J_{CF} = 3.8$, BAr^F_4), 65.84 (t, cod), 38.22 (s, C(CH_3)₂), 31.76 (s, cod), 27.04 (s, CH_3). ESI-MS (CH_2Cl_2 , 100 °C, 4.5 kV): *m/z* calc. for



Scheme 6.

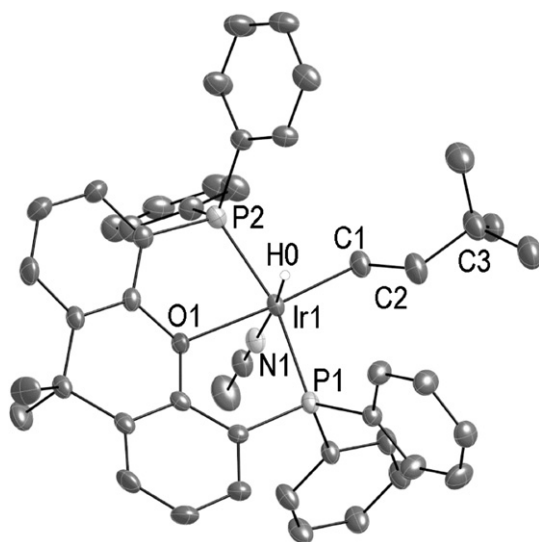


Fig. 4. Molecular crystal structure of cationic portion of **6**. Thermal ellipsoids are shown at the 30% probability level. Only the major disordered component of ^tBu and phenyl groups shown. The hydride ligand was located in the difference Fourier map. Ir1–P1, 2.2844(12); Ir1–P2, 2.2594(12); Ir–O1, 2.271(3); Ir–N1, 2.103(4); Ir1–C1, 2.086(5); C1–C2, 1.496(8); C2–C3, 1.565(7); Selected angles (°): P1–Ir1–P2, 163.43(4); O1–Ir1–N1, 89.04(12); Ir1–C1–C2, 116.8(4).

$[\text{IrP}_2\text{OC}_{47}\text{H}_{44}]^+$ 879.249, obs. 879.251. Microanalysis: calc. for $\text{C}_{79}\text{H}_{56}\text{BF}_{24}\text{OP}_2\text{Ir}$: C, 54.46; H, 3.24. Found C, 54.93; H, 3.27.

5.2. $[\text{Ir}(\kappa^3\text{-Xantphos})(\text{H})(\sigma, \eta^2\text{-C}_8\text{H}_{13})][\text{BAR}^F_4]$ **2** and $[\text{Ir}(\kappa^3\text{-Xantphos})\text{H}_2(\text{acetone})][\text{BAR}^F_4]$ **3**

A high pressure Young's NMR tube containing a d_6 -acetone (500 μl) solution of $[\text{Ir}(\text{cod})(\text{Xantphos})][\text{BAR}^F_4]$ (10 mg, 5.74×10^{-3} mmol) was placed under H_2 (~4 atm) resulting in the immediate formation of **2**, which slowly evolved over 24 h to afford **3**. Attempts to isolate a solid or crystals were unsuccessful.

5.2.1. Complex 2

^1H NMR (500 MHz, $(\text{CD}_3)_2\text{CO}$, 298 K): δ 8.18 (m, 2 H, aryl), 7.90–7.33 (m, 22H, aryl and BAR^F_4), 4.94 (m, 1H, alkene), 4.24 (m, 1H, alkene), 3.58 (s br, 1H, CH), 2.18 (m, 1H, CH_2), 1.99 (s, 3H, CH_3),

1.70 (m, 1H, CH_2), 1.41 (s, 3H, CH_3), 1.39 (m, 1H, CH_2), 1.35–1.15 (m, 3H, CH_2), 0.95 (m, 2H, CH_2), 0.58 (m, 2H, CH_2) –7.28 (dd, 1H, $J(\text{PH}) = 17.9, 27.5$). ^{31}P $\{^1\text{H}\}$ NMR (202 MHz, $(\text{CD}_3)_2\text{CO}$, 298 K): δ 7.4 (d, $J_{\text{PP}} = 288$), 3.2 (d, $J_{\text{PP}} = 288$). ESI-MS (CH_2Cl_2 , 60 °C, 4.5 kV): m/z calc. for $[\text{IrC}_{47}\text{H}_{46}\text{P}_2\text{O}_1]^+$ 881.265, obs. 881.267.

5.2.2. Complex 3

^1H NMR (500 MHz, $(\text{CD}_3)_2\text{CO}$, 298 K): δ 8.17 (m, 4H, aryl), 8.08 (dd, 2H, $J_{\text{HH}} = 7.63, 1.8, 2\text{H}$, aryl), 7.85 (s, 8H, BAR^F_4), 7.72 (m, 12H, aryl), 7.58 (m, 8H, aryl), 7.33 (m, 4H, aryl), 1.99 (s, 3H, CH_3), 1.73 (s, 3H, CH_3), –26.01 (dt, $J_{\text{HP}} = 14.8, J_{\text{HH}} = 9.0, 1\text{H}$, Ir–H), –26.90 (dt, $J_{\text{HP}} = 13.0, J_{\text{HH}} = 9.0, 1\text{H}$, Ir–H). ^{31}P $\{^1\text{H}\}$ NMR (202 MHz, $(\text{CD}_3)_2\text{CO}$, 298 K): δ 32.26 (s). ^1H $\{^{31}\text{P}\}$ NMR (500 MHz, $(\text{CD}_3)_2\text{CO}$, 298 K): δ 8.17 (d, $J_{\text{HH}} = 7.1, 4\text{H}$, aryl), 7.33 (d, $J_{\text{HH}} = 7.1, 4\text{H}$, aryl), –26.01 (d, $J_{\text{HH}} = 9.0, 1\text{H}$, Ir–H), –26.90 (d, $J_{\text{HH}} = 9.0, 1\text{H}$, Ir–H). ESI-MS (CH_2Cl_2 , 60 °C, 4.5 kV): m/z calc. for $[\text{IrC}_{42}\text{H}_{40}\text{O}_2\text{P}_2]^+$ 831.213 obs. 831.208. m/z calc. for $[\text{IrC}_{39}\text{H}_{34}\text{P}_2\text{O}]^+$ 773.171, obs. 773.168.

5.3. $[\text{Ir}(\kappa^3\text{-Xantphos})(\text{H})_2(\text{MeCN})][\text{BAR}^F_4]$ **4**

A CH_2Cl_2 solution (2 mL) of $[\text{Ir}(\text{cod})(\text{Xantphos})][\text{BAR}^F_4]$ (41.7 mg, 0.023 mmol) and CH_3CN (1.9 μl , 2 eq) was placed under H_2 (1 atm) for 24 h before placing under Ar using three freeze–pump–thaw cycles. Layering with pentane yielded colourless crystals after 48 h at –4 °C. Yield: 15.2 mg (56.8%).

^1H NMR (500 MHz, CD_2Cl_2 , 298 K): δ 7.87 (m, 4H, aryl), 7.67 (m, 12H, aryl), 7.47 (m, 22 H, aryl), 1.90 (s, 3H, CH_3), 1.55 (s, 3H, CH_3), 1.18 (s, 3H, CH_3), –18.55 (dt, $J_{\text{HP}} = 15.4, J_{\text{HH}} = 7.4, 1\text{H}$, Ir– $\text{H}_{\text{transCH}_3\text{CN}}$), –26.79 (dt, $J_{\text{HP}} = 12.8, J_{\text{HH}} = 7.37, 1\text{H}$, Ir– H_{transO}). ^{31}P $\{^1\text{H}\}$ NMR (202 MHz, CD_2Cl_2 , 298 K): δ 27.97 (s). ^1H $\{^{31}\text{P}\}$ NMR (500 MHz, CD_2Cl_2 , 298 K): δ 7.87 (d, $J = 7.0, 4\text{H}$, aryl), 7.72 (s, 8H, BAR^F_4), 7.71 (s, 2H, aryl), 7.69 (d, $J_{\text{HH}} = 1.1, 1\text{H}$, aryl), 7.57 (s, 1H, aryl), 7.55 (s, 4H, BAR^F_4), 7.54 (s, 1H, aryl), 7.52 (m, 2H, aryl), 7.51 (m, 1H, aryl), 7.47 (d, $J_{\text{HH}} = 2.2, 4\text{H}$, aryl), 7.05 (m, 4H, aryl), 7.39 (m, 6H, aryl), –18.55 (d, $J_{\text{HH}} = 7.4, 1\text{H}$), –26.79 (d, $J_{\text{HH}} = 7.4, 1\text{H}$). ESI-MS (CH_2Cl_2 , 100 °C, 4.5 kV): m/z calc. for $[\text{C}_{41}\text{H}_{37}\text{P}_2\text{NOIr}]^+$ 814.198, obs. 814.196.

5.4. $[\text{Ir}(\kappa^3\text{-Xantphos})(\text{H})(\mu\text{-H})_2][\text{BAR}^F_4]$ **5**

A fluorobenzene solution (4 mL) containing **1** (78 mg, 0.045 mmol) was placed under H_2 (4 atm) at ambient temperature for ~48 h, resulting in the formation of the product as orange

Table 1

Crystallographic data for compounds.

	1	4	5	6
CCDC	808103	808105	808104	808106
Formula	$\text{C}_{79}\text{H}_{56}\text{BF}_{24}\text{IrOP}_2$	$\text{C}_{73}\text{H}_{49}\text{BF}_{24}\text{IrNOP}_2$	$\text{C}_{142}\text{H}_{88}\text{B}_2\text{F}_{48}\text{Ir}_2\text{O}_2\text{P}_4$	$\text{C}_{79}\text{H}_{61}\text{BF}_{24}\text{IrNOP}_2$
<i>M</i>	1742.19	1677.08	3268.02	1761.24
Cryst syst	Monoclinic	Triclinic	Triclinic	Triclinic
Space group	$P2_1/n$	$P - 1$	$P - 1$	$P - 1$
<i>a</i> [Å]	15.42730(10)	14.20740(10)	12.9166(3)	12.9313(2)
<i>b</i> [Å]	22.2336(2)	15.6396(2)	17.5298(4)	18.3388(4)
<i>c</i> [Å]	21.8498(2)	18.5741(2)	18.3009(5)	18.6381(3)
α [deg]		90.6863(4)	113.8708(11)	71.7289(8)
β [deg]	107.4412(5)	108.7335(5)	94.1716(12)	70.5417(9)
γ [deg]		115.2006(6)	93.6085(11)	88.8237(8)
<i>V</i> [Å ³]	7150.01(10)	3482.81(6)	3759.85(16)	3939.95(12)
<i>Z</i>	4	2	1	2
Density [g cm ^{−3}]	1.618	1.599	1.443	1.485
μ (mm ^{−1})	2.022	2.072	1.917	1.836
θ Range [deg]	$5.11 \leq \theta \leq 26.37$	$5.10 \leq \theta \leq 26.37$	$5.11 \leq \theta \leq 26.37$	$5.10 \leq \theta \leq 26.37$
Reflns collected	14504 ($R_{\text{int}} = 0.0305$)	14147 ($R_{\text{int}} = 0.0391$)	14625 ($R_{\text{int}} = 0.0392$)	15835 ($R_{\text{int}} = 0.0313$)
No. of data/param/restr	14504/1102/224	14147/993/144	14625/1043/201	15835/1169/904
<i>R</i> 1 [<i>I</i> > 2 σ (<i>I</i>)]	0.0338	0.0401	0.0524	0.0416
<i>wR</i> 2 [all data]	0.0825	0.0875	0.1419	0.1036
GoF	1.056	1.028	1.058	1.064
Largest diff. pk and hole [e Å ^{−3}]	1.714, −1.345	2.206, −1.143	3.701, −1.530	1.378, −1.125

crystals. Yield: 38.2 mg (52.2%). Crystals suitable for X-ray diffraction were obtained by placing a concentrated dichloromethane solution of $[\text{Ir}(\text{cod})(\text{Xantphos})][\text{BAR}^{\text{F}}_4]$ under H_2 (1 atm) and layering with pentane under an atmosphere of H_2 . Pale yellow crystals were precipitated after 6 h at ambient temperature.

^1H NMR (500 MHz, CD_2Cl_2 , 298 K): δ 8.01 (dd, $J_{\text{HH}} = 7.8$, 1.12, 4H, aryl), 7.75 (s, 16H, BAR^{F}_4), 7.67 (t, $J_{\text{HH}} = 7.6$, 4H, aryl), 7.57 (s, 8H, BAR^{F}_4), 7.55 (m, 2H, aryl), 7.33 (m, 8H, aryl), 7.11 (t, 4H, $J_{\text{HH}} = 7.5$, aryl), 7.05 (t, $J_{\text{HH}} = 7.5$, 4H, aryl), 6.68 (t, $J_{\text{HH}} = 7.8$, 8H, aryl), 6.60 (t, $J_{\text{HH}} = 7.8$, 8H, aryl), 6.29 (m, 8H, aryl), 2.16 (s, 6H, CH_3), 2.14 (s, 6H, CH_3), -6.68 (m, 2H, $\text{H}_{\text{bridging}}$), -22.81 (m, 2H, $\text{H}_{\text{terminal}}$). ^{31}P $\{^1\text{H}\}$ NMR (202 MHz, CD_2Cl_2 , 298 K): δ 22.90 (s). ^1H $\{^{31}\text{P}\}$ NMR (500 MHz, CD_2Cl_2 , 298 K): δ 7.33 (dd, $J_{\text{HH}} = 8.2$, 1.1, 8H, aryl), 6.29 (dd, $J_{\text{HH}} = 8.6$, 1.1, 8H, aryl), -6.68 (t, $J_{\text{HH}} = 3.4$, 2H, $\text{H}_{\text{bridging}}$), -22.81 (t, $J_{\text{HH}} = 3.4$, 2H, $\text{H}_{\text{terminal}}$). ^{13}C $\{^1\text{H}\}$ NMR (125 MHz, CD_2Cl_2 , 298 K): 162.3 (q, $J_{\text{CB}} = 49.6$, BAR^{F}_4), 161.38 (m, aryl), 139.69 (s, aryl), 135.37 (s, BAR^{F}_4), 134.02 (m, aryl), 132.64 (s, aryl), 132.13 (s, aryl), 131.79 (s, aryl), 131.39 (br, aryl), 130.85 (s, aryl), 129.63 (m, aryl), 129.43 (qq, BAR^{F}_4), 128.91 (m, aryl), 125.10 (q, $J_{\text{CF}} = 272.7$, BAR^{F}_4), 118.04 (sep, BAR^{F}_4), 39.76 (s, $\text{C}(\text{CH}_3)_2$), 30.90 (s, CH_3), 22.69 (s, CH_3). ESI-MS (CH_2Cl_2 , 60°C, 4.5 kV): m/z calc. for $[\text{C}_{78}\text{H}_{68}\text{P}_4\text{O}_2\text{Ir}_2]^{2+}$ 773.171, obs. 773.180. Microanalysis: calc. for $\text{C}_{142}\text{H}_{92}\text{B}_2\text{F}_{48}\text{O}_2\text{P}_4\text{Ir}_2$: C, 52.12; H, 2.83. Found C, 52.99; H, 2.70.

5.5. $[\text{Ir}(\kappa^3\text{-Xantphos})(\text{MeCN})(\text{CH}_2\text{CH}_2\text{C}(\text{CH}_3)_3)(\text{H})][\text{BAR}^{\text{F}}_4]$ **6**

The (5 eq, 5 μl) was added *via* syringe to a dichloromethane solution (500 μl) containing $[\text{Ir}(\text{Xantphos})(\text{CH}_3\text{CN})_2][\text{BAR}^{\text{F}}_4]$ (11 mg, 6.6×10^{-3} mmol) in a Young's NMR tube. After 24 h the product was characterised *in situ* by NMR spectroscopy. Colourless crystals suitable for X-Ray diffraction were obtained, in low yield, by recrystallisation from $\text{CH}_2\text{Cl}_2/\text{tbe}/\text{pentane}$ at -4°C . ^1H NMR (500 MHz, CD_2Cl_2 , 298 K): δ 7.94 (m, 4H, aryl), 7.72 (s, 8H, BAR^{F}_4), 7.67 (dd, $J = 7.6$, 1.7, 2H, aryl), 7.56 (s, 4H, BAR^{F}_4), 7.63–7.28 (m, 24H, aryl), 1.91 (m, 2H, CH_2), 1.87 (s, 3H, CH_3), 1.54 (s, 3H, CH_3), 1.22 (s, 3H, CH_3CN), 0.55 (s, 9H, CH_3), -18.20 (t, $J_{\text{HP}} = 15.2$, 1H, Ir–H). ^{31}P $\{^1\text{H}\}$ (202 MHz, CD_2Cl_2 , 298 K): δ 21.34 (s). ESI-MS (CH_2Cl_2 , 60°C, 4.5 kV): m/z calc. for $[\text{IrC}_{47}\text{H}_{46}\text{P}_2\text{O}_2\text{N}]^+$ 898.290, obs 898.291.

Acknowledgements

The University of Oxford and the EPSRC for support. Dr Thomas Douglas and Romaeo Dallanegra for useful discussions.

Appendix. Supplementary material

Crystallographic data have been deposited with the Cambridge Crystallographic Data Centre under CCDC 808103–808106. These data can be obtained free of charge from The Cambridge Crystallographic Data Centre via www.ccdc.cam.ac.uk/data_request/cif

References

- [1] M. Albrecht, G. van Koten, *Angew. Chem. Int. Ed.* 40 (2001) 3750–3781.
- [2] M.E. van der Boom, D. Milstein, *Chem. Rev.* 103 (2003) 1759–1792.
- [3] D. Benito-Garagorri, K. Kirchner, *Acc. Chem. Res.* 41 (2008) 201–213.
- [4] D. Morales-Morales, C. Jensen, *The Chemistry of Pincer Compounds*. Elsevier, 2007.
- [5] P. Dierkes, P.W.N.M. van Leeuwen, *J. Chem. Soc. Dalton Trans.* (1999) 1519–1530.
- [6] P.W.N.M. van Leeuwen, P.C.J. Kamer, J.N.H. Reek, P. Dierkes, *Chem. Rev.* 100 (2000) 2741–2770.

- [7] M.-N. Birkholz, Z. Freixa, P.W.N.M. van Leeuwen, *Chem. Soc. Rev.* 38 (2009) 1099–1118.
- [8] A.E.W. Ledger, A. Moreno, C.E. Ellul, M.F. Mahon, P.S. Pregosin, M.K. Whittlesey, J.M.J. Williams, *Inorg. Chem.* 49 (2010) 7244–7256.
- [9] L.D. Julian, J.F. Hartwig, *J. Am. Chem. Soc.* 132 (2010) 13813–13822.
- [10] M.A. Zuideveld, B.H.G. Swennenhuis, M.D.K. Boele, Y. Guari, G.P.F. van Strijdonck, J.N.H. Reek, P.C.J. Kamer, K. Goubitz, J. Fraanje, M. Lutz, A.L. Spek, P.W.N.M. van Leeuwen, *J. Chem. Soc. Dalton Trans.* (2002) 2308–2317.
- [11] P. Niecypor, P.W.N.M. van Leeuwen, J.C. Mol, M. Lutz, A.L. Spek, *J. Organomet. Chem.* 625 (2001) 58–66.
- [12] A.J. Sandee, L.A. van der Veen, J.N.H. Reek, P.C.J. Kamer, M. Lutz, A.L. Spek, P.W.N.M. van Leeuwen, *Angew. Chem. Int. Ed.* 38 (1999) 3231–3235.
- [13] R.J. Pawley, G.L. Moxham, R. Dallanegra, A.B. Chaplin, S.K. Brayshaw, A.S. Weller, M.C. Willis, *Organometallics* 29 (2010) 1717–1728.
- [14] S.M. Kloek, D.M. Heinekey, K.I. Goldberg, *Organometallics* 25 (2006) 3007–3011.
- [15] W.H. Bernskoetter, S.K. Hanson, S.K. Buzak, Z. Davis, P.S. White, R. Swartz, K.I. Goldberg, M. Brookhart, *J. Am. Chem. Soc.* 131 (2009) 8603–8613.
- [16] M. Findlater, W.H. Bernskoetter, M. Brookhart, *J. Am. Chem. Soc.* 132 (2010) 4534–4535.
- [17] D. Hermann, M. Gandelman, H. Rozenberg, L.J.W. Shimon, D. Milstein, *Organometallics* 21 (2002) 812–818.
- [18] E. Ben-Ari, G. Leitun, L.J.W. Shimon, D. Milstein, *J. Am. Chem. Soc.* 128 (2006) 15390–15391.
- [19] D.J. Fox, S.B. Duckett, C. Flaschenriem, W.W. Brennessel, J. Schneider, A. Gunay, R. Eisenberg, *Inorg. Chem.* 45 (2006) 7197–7209.
- [20] A.E.W. Ledger, M.F. Mahon, M.K. Whittlesey, J.M.J. Williams, *Dalton Trans.* (2009) 6941–6947.
- [21] A.E.W. Ledger, P.A. Slatford, J.P. Lowe, M.F. Mahon, M.K. Whittlesey, J.M.J. Williams, *Dalton Trans.* (2009) 716–722.
- [22] B. Deb, B.J. Borah, B.J. Sarmah, B. Das, D.K. Dutta, *Inorg. Chem. Commun.* 12 (2009) 868–871.
- [23] J.D. Feldman, J.C. Peters, T.D. Tilley, *Organometallics* 21 (2002) 4050–4064.
- [24] M. Martin, E. Sola, O. Torres, P. Plou, L.A. Oro, *Organometallics* 22 (2003) 5406–5417.
- [25] S. Moret, R. Dallanegra, A.B. Chaplin, T.M. Douglas, R.M. Hiney, A.S. Weller, *Inorg. Chim. Acta* 363 (2010) 574–580.
- [26] C. Bianchini, E. Farnetti, M. Graziani, G. Nardin, A. Vacca, F. Zanobini, *J. Am. Chem. Soc.* 112 (1990) 9190–9197.
- [27] M.J. Fernandez, M.A. Esteruelas, L.A. Oro, M.C. Apreda, C. Foces-Foces, F.H. Cano, *Organometallics* 6 (1987) 1751–1756.
- [28] A.C. Cooper, E. Clot, J.C. Huffman, W.E. Streib, F. Maseras, O. Eisenstein, K.G. Caulton, *J. Am. Chem. Soc.* 121 (1998) 97–106.
- [29] R.H. Crabtree, *The Organometallic Chemistry of the Transition Elements*. John Wiley & Sons, New Jersey, 2005.
- [30] R.C. Schnabel, P.S. Carroll, D.M. Roddick, *Organometallics* 15 (1996) 655–662.
- [31] G.L. Moxham, H. Randell-Sly, S.K. Brayshaw, A.S. Weller, M.C. Willis, *Chem. Eur. J.* 14 (2008) 8383–8397.
- [32] K.I. Goldberg, A.S. Goldman (Eds.), *Activation and Functionalisation of C–H Bonds*, American Chemical Society, Washington, 2004.
- [33] E. Molinos, S.K. Brayshaw, G. Kociok-Kohn, A.S. Weller, *Dalton Trans.* (2007) 4829–4844.
- [34] G. Canepa, C.D. Brandt, H. Werner, *Organometallics* 23 (2004) 1140–1152.
- [35] H.E. Selnau, J.S. Merola, *Organometallics* 12 (1993) 3800–3801.
- [36] M. Kanzelberger, B. Singh, M. Czerw, K. Krogh-Jespersen, A.S. Goldman, *J. Am. Chem. Soc.* 122 (2000) 11017–11018.
- [37] M. Itazaki, C. Yoda, Y. Nishihara, K. Osakada, *Organometallics* 23 (2004) 5402–5409.
- [38] D.D. Wick, W.D. Jones, *Organometallics* 18 (1999) 495–505.
- [39] E. Ben-Ari, M. Gandelman, H. Rozenberg, L.J.W. Shimon, D. Milstein, *J. Am. Chem. Soc.* 125 (2003) 4714–4715.
- [40] X. Zhang, T.J. Emge, R. Ghosh, A.S. Goldman, *J. Am. Chem. Soc.* 127 (2005) 8250–8251.
- [41] J. Choi, Y. Choliy, X. Zhang, T.J. Emge, K. Krogh-Jespersen, A.S. Goldman, *J. Am. Chem. Soc.* 131 (2009) 15627–15629.
- [42] A.B. Pangborn, M.A. Giardello, R.H. Grubbs, R.K. Rosen, F.J. Timmers, *Organometallics* 15 (1996) 1518–1520.
- [43] J.L. Herde, J.C. Lambert, C.V. Senoff, *Inorg. Synth.* 15 (1974) 18–20.
- [44] W.E. Buschmann, J.S. Miller, K. Bowman-James, C.N. Miller, *Inorg. Synth.* 33 (2002) 83–85.
- [45] A.T. Lubben, J.S. McIndoe, A.S. Weller, *Organometallics* 27 (2008) 3303–3306.
- [46] J. Cosier, A.M. Glazer, *J. Appl. Cryst.* 19 (1986) 105–107.
- [47] Z. Otwinowski, W. Minor, *Processing of X-ray diffraction data collected in oscillation mode Pt A*, in: *Macromolecular Crystallography* (1997), pp. 307–326.
- [48] G.M. Sheldrick, *Acta Crystallogr. Sect. A* 64 (2008) 112–122.
- [49] M.C. Burla, R. Caliandro, M. Camalli, B. Carrozzini, G.L. Cascarano, L. De Caro, C. Giacovazzo, G. Polidori, R. Spagna, *J. Appl. Cryst.* 38 (2005) 381–388.
- [50] A.L. Spek, *J. Appl. Cryst.* 36 (2003) 7–13.